AFRL-RV-PS-
TR-2018-0081

AFRL-RV-PS-
TR-2018-0081

ROBUST CONSTRAINED ATTITUDE CONTROL WITH RESOURCE OPTIMAL ACTUATOR MANAGEMENT

Ufuk Topcu and Behcet Acikmese

University of Texas at Austin
101 East 27th Street, Suite 4308
Austin, TX 78712-1500

5 July 2018

Final Report

APPROVED FOR PUBLIC RELEASE; DISTRIBUTION IS UNLIMITED.

AIR FORCE RESEARCH LABORATORY
Space Vehicles Directorate
3550 Aberdeen Ave SE
AIR FORCE MATERIEL COMMAND
KIRTLAND AIR FORCE BASE, NM 87117-5776

DTIC COPY
NOTICE AND SIGNATURE PAGE

AFRL-RV-PS-TR-2018-0081 HAS BEEN REVIEWED AND IS APPROVED FOR PUBLICATION IN ACCORDANCE WITH ASSIGNED DISTRIBUTION STATEMENT.

//SIGNED//
RICHARD S. ERWIN
Program Manager

//SIGNED//
PAUL HAUSGEN
Tech Advisor, Spacecraft Component
Technology Branch

//SIGNED//
JOHN P. BEAUCHEMIN
Chief Engineer, Spacecraft Technology Division
Space Vehicles Directorate

REPORT DOCUMENTATION PAGE

Form Approved
OMB No. 0704-0188

1. REPORT DATE *(DD-MM-YYYY)*	**2. REPORT TYPE**	**3. DATES COVERED** *(From - To)*
05-07-2018	Final Report	07 Apr 2015 – 05 Jul 2018

4. TITLE AND SUBTITLE
Robust Constrained Attitude Control with Resource Optimal Actuator Management

5a. CONTRACT NUMBER

5b. GRANT NUMBER
FA9453-15-1-0303

5c. PROGRAM ELEMENT NUMBER
62601F

6. AUTHOR(S)
Ufuk Topcu and Behcet Acikmese

5d. PROJECT NUMBER
8809

5e. TASK NUMBER
PPM00020604

5f. WORK UNIT NUMBER
EF125569

7. PERFORMING ORGANIZATION NAME(S) AND ADDRESS(ES)
AND ADDRESS(ES)
University of Texas at Austin
101 East 27th Street, Suite 4308
Austin, TX 78712-1500

8. PERFORMING ORGANIZATION REPORT NUMBER

9. SPONSORING / MONITORING AGENCY NAME(S) AND ADDRESS(ES)
Air Force Research Laboratory
Space Vehicles Directorate
3550 Aberdeen Ave., SE
Kirtland AFB, NM 87117-5776

10. SPONSOR/MONITOR'S ACRONYM(S)
AFRL/RVSV

11. SPONSOR/MONITOR'S REPORT NUMBER(S)
AFRL-RV-PS-TR-2018-0081

12. DISTRIBUTION / AVAILABILITY STATEMENT
Approved for public release; distribution is unlimited.

13. SUPPLEMENTARY NOTES

14. ABSTRACT
The objective of this proposal was to develop a real-time convex optimization based methodology and onboard algorithms for constrained attitude control with optimal actuator utilization. The constrained attitude control was first planned attitude trajectories (i.e., turns) and then to execute, track, these trajectories. A challenging aspect of the constrained attitude control problems is the pointing constraints. Common pointing constraints are due to sensors that must not face the Sun and sensors that must keep lock with a relative target (e.g., point relative sensor at another spacecraft for rendezvous and point sensor at surface feature during a flyby). Another example of pointing constraints are due to plume impingement. In Formation Flying, Primitive Body Proximity Operations, and Autonomous Rendezvous and Docking, with application to on-orbit inspection), thruster plume impingement must be avoided on other spacecraft or the science site (thruster exhaust must not corrupt the surface). Furthermore there are limitations on available power/fuel and available torque, that is, overall attitude controllability is constrained. By developing robust autonomous methods to achieve the mission goals in the presence of all of the above constraints makes the constrained attitude control a challenging problem, which was the focus of the proposed research.

15. SUBJECT TERMS
Autonomous Rendezvous and Docking, AR&D, Control Moment Gyroscope, CMG, Convex Programming, CP, Formation Flying, FF, Interior Point Method, IPM, Lexicographic Goal Programming, LGP

16. SECURITY CLASSIFICATION OF:			**17. LIMITATION OF ABSTRACT**	**18. NUMBER OF PAGES**	**19a. NAME OF RESPONSIBLE PERSON**
a. REPORT	**b. ABSTRACT**	**c. THIS PAGE**			Richard S. Erwin
Unclassified	Unclassified	Unclassified	Unlimited	20	**19b. TELEPHONE NUMBER** *(include area code)*

Standard Form 298 (Rev. 8-98)
Prescribed by ANSI Std. 239.18

(This page intentionally left blank)

TABLE OF CONTENTS

(This page intentionally left blank)

1.0 SUMMARY

The research effort has focused on the problem formulations of the constrained attitude control and control allocation problems for spacecraft, and their incorporation into trajectory optimization. This has included the mathematical formulation of the constrained attitude control problem, mathematical formulation of control allocation methods, developing offline algorithms for numerical solutions, and developing custom interior point methods (IPMs) for solving second order cone programs (SOCPs). To allow fast computations, the mathematical formulation of the constrained attitude control problem involves the convexification of state constraints due to pointing and unity quaternions, convexification of kinematics and dynamics, and trajectory refinement. For the formulation of control allocation methods, we developed a single time-step allocation method via lexicographic goal programming formulations. We have developed cost metrics for Reaction Wheel Assembly (RWA) and Control Moment Gyro (CMG) power consumption. Also, we have developed a set of priorities for expected failure modes.

With non-convex problems formulated, methods for solving these problems are required. We have developed general purpose algorithms for solving non-linear optimal control problems. Software has been developed to use these algorithms and solve SOCP problems for both attitude motion planning and control allocation problems.

2.0 INTRODUCTION

The main mathematical problem formulated is the so called constrained attitude guidance (CAG) problem. Natural constraints to include angular rate constraints and conic exclusion regions (i.e. pointing constraints). This allows, for example, preventing a sensitive instrument from being compromised by the sun. The CAG problem is solved by considering only the quaternion kinematics in the formulation and using constraints on quaternions and their time derivatives to indirectly apply bounds on the angular rates and accelerations [1]. The CAG formulation we introduce makes use of Mixed Integer Convex Programming (MICP) to impose, approximately, the unity constraint on the quaternion magnitude, where the approximation accuracy can be set to a desired accuracy. The solution complexity of the MICP formulation increases exponentially with the number of binary variables that are used to impose the unit norm constraint on the quaternion. Since this number is independent of the number of exclusion pointing constraints, the solution approach has favorable complexity in terms of the number of pointing constraints. Commercial MICP solvers, such as Gurobi, are used to test the viability of the formulation.

For the control allocation problem, we considered the setting of optimally utilizing multiple actuators on a momentum control system while explicitly considering actuator constraints. The primary objective of the allocation is to minimize torque error and improve performance when the system saturates or becomes singular. As a secondary objective, internal bearing and gear friction are exploited to reduce power usage without the need for accurate friction models. We formulated a greedy allocation problem (i.e., optimal allocation by using the current conditions and needs alone) as a convex optimization problem, specifically as a lexicographic Second Order Cone Programming problem (SOCP) [2]. The algorithm exploits the fact that redundant control moment gyroscopes (CMGs) and the rotors of reaction wheel assemblies (RWAs) have nonsingleton minimum torque error solutions. Thus, friction in the rotors and gimbals of the CMGs and RWA can be used to find a minimum power solution among the set of minimum torque error solutions. The convex optimization framework enables real-time implementable algorithms, which fully utilize control authority without requiring tuning for changes in the number or the configuration of actuators. This formulation is shown to be highly effective in improving the robustness and performance of the CMGs operation in comparison to earlier algorithms in the literature.

Work has also been towards developing general algorithms which solve the non-convex optimal control problems that arise from the above formulations. These algorithms fall into the category of Successive Convexification (SCVx). Work has been done on using different options in SCvx for different sources of non-convexities. For example, we have studied synthesizing virtual control inputs together with thrust regions [3] to ensure feasibility during SCvx iterations and considered a linearize-and-project approach to handle non-convex state constraints [4]. These approaches gave very good initial results, and we are now working on combining these methods.

Many of these algorithms have been tested on quadrotors in our laboratory, Autonomous Control Laboratory (ACL), at University of Washington (UW). This is enabled by the development of custom IPMs. The following link has the videos of some the flight experiments (both single and multiple vehicle scenarios).

https://www.youtube.com/channel/UCZwV0cPCR3QeGn4dSfXxkKw

The single vehicle flight experiments are performed by using our in-house built custom quadrotor, and the trajectories used SCvx algorithm, particularly in collision avoidance scenarios [5].

The SCvx algorithm is executed onboard in real-time, by using our in-house developed custom IPM numerical solvers [6] to compute optimal solutions of the resulting Second-Order-Cone-Programming (SOCP) problems.

Experiments have demonstrated multi-obstacle avoidance for both static and dynamic obstacles. The lab now has the capabilities to test multivehicle algorithms. Such tests will be conducted in the near future.

3.0 METHODS, ASSUMPTIONS AND PROCEDURES

3.1 CONSTRAINED ATTITUDE GUIDANCE PROBLEM

The objective of the specific Constrained Attitude Guidance problem we considered is to find a quaternion time history, q(t), over a time interval [t_0; t_f] that is subject to initial/ final state conditions, pointing constraints, and angular rate constraints. The quaternion and angular velocity vectors are partitioned into components as follows,

$$\begin{aligned} q(t) &= [\mu(t), \epsilon(t)], \\ \omega(t) &= [\omega_1(t), \omega_2(t), \omega_3(t)] \end{aligned} \tag{1}$$

Here, μ(t) in R^3 represents the vector part of the quaternion while ε(t) stands for the scalar component. When the body coordinate system for the vehicle is aligned with the principal axes of inertia, the attitude dynamics can be expressed as

$$\begin{aligned} J_1\dot{\omega}_1(t) - (J_2 - J_3)\omega_2(t)\omega_3(t) &= u_1(t), \\ J_2\dot{\omega}_2(t) - (J_3 - J_1)\omega_3(t)\omega_1(t) &= u_2(t), \\ J_3\dot{\omega}_3(t) - (J_1 - J_2)\omega_1(t)\omega_2(t) &= u_3(t), \end{aligned} \tag{2}$$

where J_i , i = 1,2,3 are the principle moments of inertia of the vehicle, ω_i are the components of the angular velocity vector about the principal axes and μ_i are the control torques. The following is the expression for the quaternion rate, where we note that its associated dynamics are norm preserving, i.e., $\|q(t)\| = 1$:

$$\dot{q}(t) = \frac{1}{2}\Omega(\omega(t))q(t) \tag{3}$$

Here, $(\Omega(t))$ is a skew-symmetric matrix that is a function of the angular velocity vector:

$$\Omega(\omega(t)) = \begin{bmatrix} 0 & \omega_3(t) & -\omega_2(t) & \omega_1(t) \\ -\omega_3(t) & 0 & \omega_1(t) & \omega_2(t) \\ \omega_2(t) & -\omega_1(t) & 0 & \omega_3(t) \\ -\omega_1(t) & -\omega_2(t) & -\omega_3(t) & 0 \end{bmatrix} \tag{4}$$

Along with these dynamics, we must also ensure that the angular velocity and acceleration vectors are sufficiently bounded in order to impose the control authority constraints, as well as the state constraints due to mission considerations:

$$\left.\begin{array}{l} \|\omega(t)\| \leq \delta_1 \\ \|\dot{\omega}(t)\| \leq \delta_2 \end{array}\right\} \quad \forall\, t \in [t_0, t_f]. \tag{5}$$

Finally, pointing constraints are enforced to protect sensitive on-board instruments by avoiding predefined conic regions, see [7] for the details of the formulation. This type of conic exclusion zone can be defined with the following non-convex quadratic constraint:

$$q(t)^{\mathrm{T}} P_i(x_i, y_i, \theta_i) q(t) \leq 0, \quad i = 1, \ldots, m, \tag{6}$$

where the inequality given in (6) defines m number of conic exclusion zones by expressing them as m number of non-convex quadratic constraints, and,

$$\begin{gathered} P_i(x_i, y_i, \theta_i) = \begin{bmatrix} A_i & b_i \\ b_i^{\mathrm{T}} & d_i \end{bmatrix} \in \mathbb{R}^{4\times 4} \\ A_i := x_i y_i^{\mathrm{T}} + y_i x_i^{\mathrm{T}} - \left(x_i^{\mathrm{T}} y_i + \cos\theta_i\right) I_3 \\ b_i := -x_i \times y_i, \qquad d_i := x_i^{\mathrm{T}} y_i - \cos\theta_i, \end{gathered} \tag{7}$$

where x_i defines the direction of the i^{th} sensitive instrument in the body frame, y_i defines the center of the i^{th} conic exclusion zone, and θ_i represents the half cone angle about y_i. Now the CAG problem can be written as:

Compute $q(t)$, !(t), and $u(t)$ over t in [t_0; t_f] such that

$$q(t_0)=q_0, \quad \omega(t_0)=\omega_0, \quad q(t_f)= q_f, \quad \omega(t_f)=\omega_f, \tag{8}$$

and the conditions (2, 3, 5, 6) hold for all [t_0; t_f]. This problem has both non-linear dynamics as well as a non-convex quadratic pointing constraint. Therefore, relaxations are required to solve the problem in a convex optimization framework. since attitude quaternions are unit vectors (that is, $||q(t)|| = 1$ for all t in [t_0; t_f]), the inequalities in (6) can be converted into the form given below:

$$\left.\begin{aligned} q(t)^{\mathrm{T}}\hat{P}_i(x,y,\theta)q(t) \le l_i, \\ \hat{P}_i = P_i + l_i I_4 \end{aligned}\right\} \quad i = 1, ..., m \tag{9}$$

where l_i is any positive real number which is greater than the smallest (most negative) eigenvalue of P_i. Essentially, the pointing constraints are converted into semi-definite constraints by shifting the spectrum of the P_i matrices. The full non-linear dynamics are also not imposed and instead we impose constraints on the first and second time derivatives of the quaternions. Bounding these rates implies bounds on the control authority, and hence the resulting trajectories are still dynamically feasible. To that end, we first discretize the quaternion time derivatives and impose all the constraints on the discretized variables. Then we solve a convex optimization problem to obtain a feasible quaternion history sampled at finite number of time instances. The quaternions between consecutive samples are used to compute the actual angular velocity vector by assuming constant acceleration between the time samples, see [1] for details. Another non-convexity is the bounds on angular velocity and acceleration which are handled by the following lemmas.

Lemma 1: The magnitude of angular velocity vector $||\ \omega(t)\ ||$ can be bounded by bounding the magnitude of the quaternion rates $||\dot{q}(t)||$ as:

$$\|\dot{q}(t)\| \le \bar{\omega} \;\Rightarrow\; \|\omega(t)\| \le 2\bar{\omega}. \tag{10}$$

Lemma 2: The magnitude of angular acceleration vector $||\dot{\omega}(t)\ ||$ can be bounded by bounding the magnitude of the quaternion rates $||\ddot{q}(t)||$ as:

$$\|\ddot{q}(t)\| \le \bar{\alpha} \;\Rightarrow\; \sqrt{\|\dot{\omega}(t)\|^2 + \frac{\|\omega(t)\|^4}{4}} \le 2\bar{\alpha}. \tag{11}$$

Both results can be proved by manipulating (3). Finally, the constraint of quaternion unity is itself non-convex and therefore must be convexified. This is accomplished with a set bounding hyperplanes. An arbitrary number of such hyperplanes can be used to approximate the quaternion space to an arbitrary degree. Introducing hyperplane constraints and performing a time discretization on the dynamics requires the introduction of binary variables in order to satisfy the constraints. See [1] for specific details, but the overall problem can be expressed as:

$$\min_{q, z_{ik}} \sum \|\ddot{q}_k\| \qquad \text{s.t} \tag{12}$$

$$\epsilon_k \geq 0, \qquad k = 0, \ldots, N \tag{13}$$

$$\|\dot{q}_k\| \leq \bar{\omega}, \qquad \|\ddot{q}_k\| \leq \bar{\alpha}, \qquad k = 0, \ldots, N \tag{14}$$

$$q_k^{\mathrm{T}} \hat{P}_i(x, y, \theta) q_k \leq b, \quad i = 1, \ldots, n_c, \qquad k = 0, \ldots, N \tag{15}$$

$$q_k = [\mu_{1k}, \mu_{2k}, \mu_{3k}, \epsilon_k]^{\mathrm{T}} \qquad k = 0, \ldots, N \tag{16}$$

$$\dot{q}_k = \{q_{k+1} - q_{k-1}\}/2\Delta t, \qquad k = 1, \ldots, N-1 \tag{17}$$

$$\ddot{q}_k = \{q_{k+1} - 2q_k + q_{k-1}\}/\Delta t^2, \qquad k = 1, \ldots, N-1 \tag{18}$$

$$q_0 = \nu_0, \qquad q_N = \nu_N \tag{19}$$

$$\dot{q}_0 = \dot{\nu}_0, \qquad \dot{q}_N = \dot{\nu}_N \tag{20}$$

$$\ddot{q}_0 = \{q_1 - q_0\}/(0.5\Delta t)^2, \tag{21}$$

$$\ddot{q}_N = \{q_N - q_{N-1}\}/(0.5\Delta t)^2, \tag{22}$$

$$S_i q_k \leq 1 + M z_{ik}, \quad i = 1, \ldots, n_p, \qquad k = 0, \ldots, N \tag{23}$$

$$S_i q_k \geq 1 - M z_{ik}, \quad i = 1, \ldots, n_p, \qquad k = 0, \ldots, N \tag{24}$$

$$\sum_{i=1}^{n_p} z_{ik} \leq n_p - 1 \tag{25}$$

$$z_{ik} \in \{0, 1\} \tag{26}$$

This formulation can be solved to global optimality using commercial solvers.

3.2 CONTROL ALLOCATION PROBLEM

For the control allocation problem, we developed a technique called Minimum Error Dissipative Power Reduction Control (ME-DPRC). We have considered a spacecraft with n CMGs and n RWA is summarized; details can be found in [8]. As in [8], we assume that (i) the carrier body, and the gimbal and rotor Center-of-Masses (CMs) are fixed in the spacecraft body frame; (ii) the gimbal and rotor CMs coincide at the origin of their corresponding CMG frame, which is also assumed to have its origin along the gimbal axes where the rotor and gimbal axes intersect; (iii) the rotor spin axis is orthogonal to the gimbal axis; (iv) the rotor angular momentum is uniform across all CMGs; (v) the rotor and gimbal wheel assembly inertias are uniform across all CMGs and RWA. Therefore, the approximate equations of motion for the spacecraft-CMG system are given by,

$$\mathbf{I}^S \dot{\boldsymbol{\omega}} + \boldsymbol{\omega}^{\times} \mathbf{I}^S (\boldsymbol{\omega} + \boldsymbol{h}) + \dot{\boldsymbol{h}} = \boldsymbol{\tau}_{ext}, \tag{27}$$

where I^S is the spacecraft inertia matrix about the CM and ω is the spacecraft angular velocity matrix in body coordinates, h is the sum of actuator angular momenta (e.g., due to CMGs) in body coordinates, h– is the angular velocity provided by the actuator, e.g., $\dot{h} = h_0 A_t \dot{\delta}$ is the internal torque contribution of the CMGs, $h_0 = I^{W}\dot{s}$ is the nominal rotor angular momentum, and $_{ext}$ are external torques. For spacecraft equipped with an array of n RWAs, the gimbals are stationary, but the rotors do not have constant rates, so $\dot{h} = I^{W}s\ A_s\ \dot{\Omega}$. In the above formulations, is the vector of rotor rotational rates, and $\dot{\delta}$ is the vector of gimbal rates.

Assuming that the rotor and gimbal motors are stiff, the equations of motion for the rotor and gimbal angles can be found by taking the spin and gimbal axes projection as in [8], including the friction torque, τ_f , and the commanded torque, τ_c: For i = ,…, n, where n is the number of CMGs or RWAs,

$$\dot{\Omega}_i = -\frac{1}{I^{W_{s,i}}}\left(\tau_{Wci} - \tau_{Wfi}\right), \quad \text{and} \tag{28}$$

$$\ddot{\delta}_i = -\frac{1}{I^{GW_{g,i}}}\left(I^{W_{s,i}}\Omega_i\omega_{t,i} + \tau_{Gci} - \boldsymbol{\tau}_{Gfi}\right). \tag{29}$$

Combining the equations above, the equations of motion for a spacecraft with n CMGs are given by equations (27) and (29), and with RWAs the equations are given by (27) and (28). A friction torque model was used which exhibits the so-called “bathtub curve" behavior where friction is lowest in the middle of the operating velocity range. See [2] for the model used, or [9] for high fidelity friction models. Control allocation typically lies below a higher tier spacecraft controller that generates torque commands, but above inner loop controllers that regulate gimbal and rotor rates.

Following the results in [2], we find that the minimum torque errors found using a Moore-Penrose (MP) pseudo inverse method for CMGs and RWAs respectively can be expressed as:

$$\dot{\boldsymbol{\delta}}^*_{k+1} = \frac{1}{h_0}(\mathbf{A}_k^{\mathrm{T}}\mathbf{A}_k)^{-1}\mathbf{A}_k^{\mathrm{T}}\,\dot{\boldsymbol{h}}_{des,k}. \tag{30}$$

and,

$$\dot{\boldsymbol{\Omega}}^*_{k+1} = \frac{1}{I^W}(\mathbf{A}_s^{\mathrm{T}}\mathbf{A}_s)^{-1}\mathbf{A}_s^{\mathrm{T}}\dot{\boldsymbol{h}}_{des,k}, \tag{31}$$

the analytic solution shown above, the allocation can be done using optimization. Both the allocation for the RWAs and CMGs t into a Lexicographical Goal Programming (LGP) framework. LGP is a setting where multiple optimization objectives are sorted such that one can first solve the optimization problem involving the most important cost function. Then that optimal cost is used as a constraint for the remainder of the optimizations. This is repeated for all remaining costs. For our setting the primary objective is to minimize the torque error and the secondary objective is to minimize the power consumption subject to enforcing a minimum torque. The specific optimization problems obtained are:

$$\min_{\boldsymbol{\Omega}_{k+1},\dot{\boldsymbol{\Omega}}_k} J_1 = \left\|\dot{\boldsymbol{h}}_{des,k} - I^W\mathbf{A}_s\dot{\boldsymbol{\Omega}}_k\right\|_1, \ \text{s.t. (33)}, \tag{32}$$

where

$$\begin{gathered}\boldsymbol{\Omega}_{k+1} = \boldsymbol{\Omega}_k + \dot{\boldsymbol{\Omega}}_k\Delta t,\\ -\boldsymbol{\Omega}_{max} \le \boldsymbol{\Omega}_{k+1} \le \boldsymbol{\Omega}_{max}, \quad -\dot{\boldsymbol{\Omega}}_{max} \le \dot{\boldsymbol{\Omega}}_k \le \dot{\boldsymbol{\Omega}}_{max},\end{gathered} \tag{33}$$

For the minimum RWA error and,

$$\min_{\boldsymbol{\Omega}_{k+1},\dot{\boldsymbol{\Omega}}_k} J_2 = \left\| \left(I^W \dot{\boldsymbol{\Omega}}_k - \boldsymbol{\tau}_{fW,k} \right) \odot \boldsymbol{\Omega}_k \right\|_1 , \\ \text{s.t.} \left\| \dot{\boldsymbol{h}}_{des,k} - I^W \mathbf{A}_s \dot{\boldsymbol{\Omega}}_k \right\|_1 \leq J_1^*, \quad (33) \ , \tag{34}$$

For the RWA power consumption. Similarly, for the CMGs,

$$\min_{\dot{\boldsymbol{\delta}}_{k+1},\ddot{\boldsymbol{\delta}}_k} J_1 = \left\| \dot{\boldsymbol{h}}_{des,k} - h_0 \mathbf{A}_{k+1} \dot{\boldsymbol{\delta}}_{k+1} \right\|_2 \ \text{s.t.}, \ (36), \tag{35}$$

with

$$\dot{\boldsymbol{\delta}}_{k+1} = \dot{\boldsymbol{\delta}}_k + \ddot{\boldsymbol{\delta}}_k \Delta t, \\ -\dot{\boldsymbol{\delta}}_{max} \leq \dot{\boldsymbol{\delta}}_{k+1} \leq \dot{\boldsymbol{\delta}}_{max}, \quad -\ddot{\boldsymbol{\delta}}_{max} \leq \ddot{\boldsymbol{\delta}}_k \leq \ddot{\boldsymbol{\delta}}_{max}, \tag{36}$$

Is the problem for the minimum torque error and,

$$\min_{\dot{\boldsymbol{\delta}}_{k+1},\ddot{\boldsymbol{\delta}}_k} J_2 = \left\| \left(I_{gw} \ddot{\boldsymbol{\delta}}_k - h_0 \hat{\mathbf{A}}_k^{\mathrm{T}} \boldsymbol{\omega}_k - \boldsymbol{\tau}_{fG,k} \right) \odot \dot{\boldsymbol{\delta}}_{k+1} \right\|_1 \ \text{s.t.} \ (36), \\ \left\| \dot{\boldsymbol{h}}_{des,k} - h_0 \hat{\mathbf{A}}_k \dot{\boldsymbol{\delta}}_{k+1} \right\|_2 \leq J_1^*, \tag{37}$$

Is the minimum power problem. See [2] for specifics, especially for notation and additional assumptions imposed for the problems.

3.3 SUCCESSIVE CONVEXIFICATION

In addition to working on specific attitude control and control allocation problems, we have worked on developing algorithms that solve general nonlinear control problems. We call this family of methods successive convexification. The main results can be found in [3][4]. We can consider the general discrete time optimal control problem:

$$\min J(x_i, u_i) := \sum_{i=1}^{T} \phi(x_i, u_i) \tag{38}$$

subject to

$$x_{i+1} - x_i = f(x_i, u_i) \qquad i = 1, 2, \ldots, T-1 \tag{39}$$

$$h(x_i) \geq 0 \qquad i = 1, 2, \ldots, T \tag{40}$$

$$u_i \in \mathcal{U}_\rangle \subseteq \mathbb{R}^m \qquad i = 1, 2, \ldots, T-1 \tag{41}$$

$$x_i \in \mathcal{X}_\rangle \subseteq \mathbb{R}^n \qquad i = 1, 2, \ldots, T \tag{42}$$

Where x_i, u_i represent discrete states and controls at each time point, T denotes the final time and X_i, U_i are assumed to be convex and compact sets. We also assume that the objective function is continuous and convex. For convergence of the algorithms it is assumed that the dynamics function $f(x_i; u_i)$ is convex over its arguments. In addition, it is assumed that each component of $h(x_i)$ is convex.

The main idea behind successive convexification algorithms is to iteratively solve a relaxed version of the true problem around an existing trajectory. The relaxed problem is generally a linearization of the non-convex constraints in the original problem. This linearization can be done either directly around a trajectory (potentially infeasible) using the results in [3]. Or the linearization can be done about a projection onto the infeasible space using the results in [4]. Variations on the algorithm have been explored, particularly investigating convergence properties and means to deal with a variety of constraints [10], [11].

4.0 RESULTS AND DISCUSSION

All of the results of the work have been demonstrated with numerical simulations. In addition, many results have been tested on our laboratory on quadrotors. The results for the constrained attitude control problem were demonstrated for a spacecraft with inertia matrix along the principle axes. Parameter values can be found in [1]. An example of a trajectory which satisfies the given constraints is shown in figure 1. This depicts two avoidance cone regions in blue and green as well as the motion of the body vectors $x_1 = [0; 0; 1]^T$ and $x_2 = [1; 0; 0]^T$ in the inertial frame and the motion of the body vector $e_2 = [0; 1; 0]^T$ in dotted blue, green, and black lines respectively. With this mixed integer approach, there is an exponential increase in complexity with the number of binary variables. However, since the binary variables are solely used to impose the unity quaternion constraint, adding more attitude exclusion cone constraints does not introduce any new binary variables, hence the solution complexity does not increase exponentially with the number of exclusion constraints.

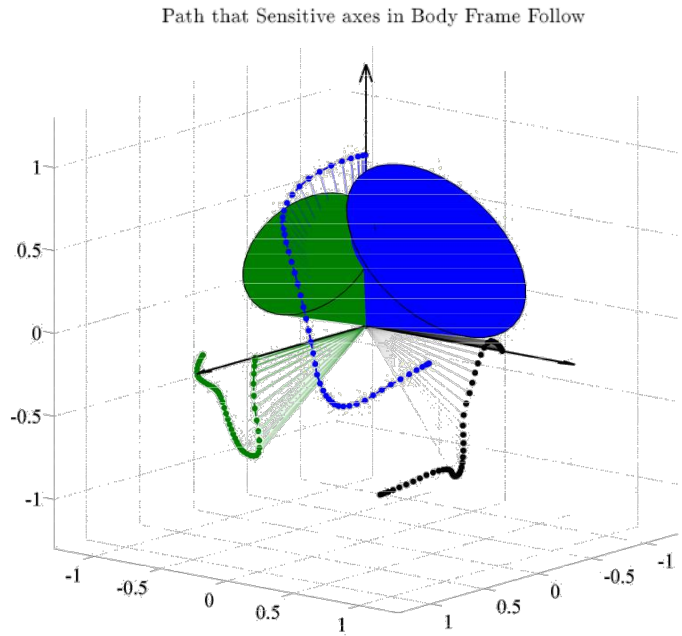

Figure 1. Path That Directions of Sensitive Instruments in Body Frame Follow

The control allocation results were also demonstrated for an allocation given feed-forward open loop control torques. Both linear and sinusoidal torque tracking were tested for the RWA, and a single axis slew as well as high-amplitude sinusoidal torque tracking were tested for the CMGs. The analytic Moore-Penrose (MP) pseudo-inverse solutions are compared to our optimization-based solutions. The optimization-based solution is able to continue tracking desired torques after the MP solution starts degrading because of its ability to explicitly handle constraints. In addition, it is able to save power.

The real-time implementation of ME-DPRC is important to note. The custom solvers are used for both RWA and CMG examples, which show 0.2 ms (5000 Hz update rate) computation time per allocation on a laptop with 2.1 GHz Intel i7 processor and 8 GB of RAM. - making ME-DPRC real-time implementable. Customized solvers were recently demonstrated on a NASA test flight, where optimal landing trajectories were generated in real-time onboard the rocket's flight computer [12, 13]. These show a considerable level of flight readiness of the custom IPMs. We have also formalized convergence proofs for the various successive convexification methods. In particular proofs of properties such as local optimality, global convergence, and superlinear convergence have been developed [3][4][10].

The successive convexification algorithms have successfully been tested on the quadrotors in our laboratory. The algorithms have been implemented on board embedded processors and are able to solve motion planning problems in real time thanks to custom interior point method solvers.

The most recent result comes from [5]. This paper demonstrated that numerical optimization techniques based on convex optimization are well-suited for applications that require real-time on-board motion planning in the presence of non-convexities. An agile flip maneuver that required the use of non-convex control constraints was planned on-board the vehicle in real-time via lossless convexification. Also, it was demonstrated that a quad-rotor could compute trajectories that avoid cylindrical obstacles by utilizing successive convexification techniques.

5.0 CONCLUSIONS

Successful results have been obtained on a variety of problems, primarily including the constrained attitude control and control allocation problems for spacecraft, and their incorporation into trajectory optimization. The mathematical formulations were developed as well as algorithms for numerical solutions. This includes developing custom methods intended for real-time implementation. Techniques were developed for convexifying non-convex constraints such that problems could be solved to global optimality with guarantees. Many of the ideas and algorithms developed have been implemented on quadrotors in our laboratory.

REFERENCES

[1] Utku Eren, Behcet Ackmese, and Daniel P Scharf, “A mixed integer convex program-ming approach to constrained attitude guidance,” *Proceedings of European Control Conference (ECC)*, Linz, Austria, pp. 1120-1126, 2015.

[2] Daniel Dueri, Frederick Leve, and Behcet Ackmese, “Minimum error dissipative power reduction control allocation via lexicographic convex optimization for momentum control systems,” IEEE Transactions on Control Systems Technology, 24(2), pp. 678-686, 2016.

[3] Yuanqi Mao, Michael Szmuk, and Behcet Ackmese, “Successive convexification of non-convex optimal control problems and its convergence properties,” *Proceedings of IEEE 55th Conference on Decision and Control*, Las Vegas, NV, pp. 3636-3641, 2016.

[4] Yuanqi Mao, Daniel Dueri, Michael Szmuk, and Behcet Ackmese, “Successive convexication of non-convex optimal control problems with state constraints,” IFAC-PapersOnLine, 50(1), pp. 4063-4069, 2017.

[5] Michael Szmuk, Carlo Alberto Pascucci, Daniel Dueri, and Behcet Acikmese, “Convexication and real-time on-board optimization for agile quad-rotor maneuvering and obstacle avoidance,” *2017 IEEE/RSJ International Conference on Intelligent Robots and Systems*, Vancouver, Canada, pp. 4862-4868, 2017.

[6] Daniel Dueri, Jing Zhang, and Behcet Acikmese, “Automated custom code generation for embedded, real-time second order cone programming,” IFAC Proceedings Volumes, 47(3), pp. 1605-1612, 2014.

[7] Y. Kim and M. Mesbahi, “Quadratically constrained attitude control via semidefinite programming,” IEEE Transactions on Automatic Control, 49(5), pp. 633-863, May 2004.

[8] H. Schaub, S.R. Vadali, and J.L. Junkins, “Feedback Control Law for Variable Speed Control Moment Gyros,” Journal of the Astronautical Sciences, 46(3), pp. 307-328, 1998.

[9] EJ Berger, “Friction modeling for dynamic system simulation,” Applied Mechanics Reviews, 55(6), pp. 535-577, 2002.

[10] Yuanqi Mao, Michael Szmuk, and Behcet Acikmese, “Successive convexification: A superlinearly convergent algorithm for non-convex optimal control problems,” arXiv preprint arXiv:1804.06539, Seattle, WA, 2018.

[11] Daniel Dueri, Yuanqi Mao, Zohaib Mian, Jerry Ding, and Behcet Acikmese, "Trajectory optimization with inter-sample obstacle avoidance via successive convexification," *Proceedings of 2017 IEEE 56th Annual Conference on Decision and Control*, Melbourne, Australia, pp. 1150-1156, 2017.

[12] B. Ackmese et al., "Flight testing of trajectories computed by G-FOLD: Fuel optimal large divert guidance algorithm for planetary landing," *In AAS/AIAA Spacefight Mechanics Meeting*, Kauai, Hawaii, 2013.

[13] D. P. Scharf, et al., "ADAPT demonstrations of onboard large-divert guidance with a reusable launch vehicle," *IEEE Aerospace Conference*, Big Sky, Montana, 2014.

LIST OF SYMBOLS, ABBREVIATIONS, AND ACRONYMS

ACL	Autonomous Controls Laboratory
(AR&D)	Autonomous Rendezvous
CAG	Constrained Attitude Guidance
CMG	Control Moment Gyroscope
CMs	Center-of-Masses
CP	Convex Programming
FF	Formation Flying
IPM	Interior Point Method
LGP	Lexicographical Goal Programming
ME-DPRC	Minimum Error Dissipative Power Reduction Control
MICP	Mixed Integer Convex Programming
MP	Moore-Penrose
NASA	National Aeronautics and Space Administration
PB-ProxOps	Primitive Body Proximity Operations
RWA	Reaction Wheel Assembly
SCVx	Successive Convexification
SOCPs	Second Order Cone Programs
UW	University of Washington

DISTRIBUTION LIST

DTIC/OCP 8725 John J. Kingman Rd, Suite 0944 Ft Belvoir, VA 22060-6218	1 cy
AFRL/RVIL Kirtland AFB, NM 87117-5776	1 cy
Official Record Copy AFRL/RVSV/Richard S. Erwin	1 cy